



LAWRENCE
LIVERMORE
NATIONAL
LABORATORY

Prediction of heat transfer coefficients for forced convectiveboiling of N2-Hydrocarbon mixtures at cryogenic conditionsusing artificial neural networks

J. M. Barroso-Maldonado, J. M. Belman-Flores, S. Ledesma, S. M. Aceves

February 1, 2018

Cryogenics

Disclaimer

This document was prepared as an account of work sponsored by an agency of the United States government. Neither the United States government nor Lawrence Livermore National Security, LLC, nor any of their employees makes any warranty, expressed or implied, or assumes any legal liability or responsibility for the accuracy, completeness, or usefulness of any information, apparatus, product, or process disclosed, or represents that its use would not infringe privately owned rights. Reference herein to any specific commercial product, process, or service by trade name, trademark, manufacturer, or otherwise does not necessarily constitute or imply its endorsement, recommendation, or favoring by the United States government or Lawrence Livermore National Security, LLC. The views and opinions of authors expressed herein do not necessarily state or reflect those of the United States government or Lawrence Livermore National Security, LLC, and shall not be used for advertising or product endorsement purposes.

Prediction of heat transfer coefficients for forced convective boiling of N₂-Hydrocarbon mixtures at cryogenic conditions using artificial neural networks

J.M. Barroso-Maldonado^{1*}, J.M. Belman-Flores¹, S. Ledesma¹, S.M. Aceves²

¹ *Engineering Division, Irapuato-Salamanca Campus, University of Guanajuato, Salamanca, Gto, 36885, Mexico.*

² *Lawrence Livermore National Laboratory, Livermore, CA, 94550, USA.*

* Corresponding author.

Tel.: +52 (464) 6479940 Ext. 2419; fax: +52 (464) 6479940 Ext. 2311

E-mail address: jm.barrosomaldonado@ugto.mx (J.M. Barroso-Maldonado)

Abstract

A key problem faced in the design of heat exchangers, especially for cryogenic applications, is the determination of convective heat transfer coefficients in two-phase flow such as condensation and boiling of non-azeotropic refrigerant mixtures. This paper proposes and evaluates three models for estimating the convective coefficient during boiling. These models are developed using computational intelligence techniques. The performance of the proposed models is evaluated using the mean relative error (*mre*), and compared to two existing models: the modified Granryd's correlation and the Silver-Bell-Ghaly method. The three proposed models are distinguished by their architecture. The first is based on directly measured parameters (DMP-ANN), the second is based on equivalent Reynolds and Prandtl numbers (eq-ANN), and the third on effective Reynolds and Prandtl numbers (eff-ANN).

The results demonstrate that the proposed artificial neural network (ANN)-based approaches greatly outperform available methodologies. While Granryd's correlation predicts experimental data within a mean relative error *mre*=44% and the S-B-G method produces *mre*=42%, DMP-ANN has *mre*=7.4% and eff-ANN has *mre*=3.9%. Considering that eff-ANN has the lowest mean relative error (one tenth of previously available methodologies) and the broadest range of applicability, it is recommended for future calculations. Implementation is straightforward within a variety of platforms and the matrices with the ANN weights are given in the appendix for efficient programming.

Keywords: heat transfer coefficient; boiling; heat exchangers, cryogenics; artificial intelligence.

Nomenclature

A	Area
C_p	Specific heat
D	Diameter
G	Mass flux
h	Convective heat transfer coefficient
i	Enthalpy
k	Thermal conductivity
$LMTD$	Logarithmic mean temperature difference
mre	Mean relative error
MW	Molecular weight
Nu	Nusselt number
P	Pressure
Pr	Prandtl number
\dot{q}	Heat flux
Re	Reynolds number
T	Temperature
U	Global heat transfer coefficient
x	Quality
w	Weights of the ANN

Greek symbols

α	ANN input vector
----------	------------------

β ANN output
 ε Linear accumulation
 δ Actual weights of the ANN
 θ Number of neurons in the hidden layer
 μ Dynamic viscosity
 ρ Density

Subscripts

dew Dew point
eff Effective
eq Equivalent
k Target neuron
l Liquid phase
v Vapor phase

1. Introduction

Liquefaction enables effective storage and worldwide distribution of natural gas without the need for capital intensive pipelines. Research on this important topic is therefore well warranted [1] as natural gas liquefaction is an energy intensive process.

Liquefaction is typically conducted in thermodynamic cycles based on vapor compression technology. In the search for energy performance improvements, different modifications have been proposed to the basic vapor compression system, and three main approaches are available for natural gas liquefaction: isentropic expansion based processes, cascade processes, and mixed refrigerant processes (MR). The MR process uses a non-azeotropic mixture of nitrogen, ethane, propane, butane and pentane as refrigerant. Some technologies based on mixed refrigerants are: single mixed refrigerant process (SMR) and mixed refrigerant with propane pre-cooling (C3/MR).

Condensation and boiling heat transfer of mixed refrigerant systems are critical to the performance of MR liquefaction units, as this will determine heat exchanger dimensions and system performance. Many factors affect MR heat transfer including inlet and outlet stream temperatures, operating pressures, mass flow rates, as well as the molecular composition of the refrigerant and natural gas. In this sense, the literature shows the complexity that this represents because of the presence of a large number of degrees of freedom that are involved in the sizing of a liquefaction plant [2].

Aside from system complexity, estimation of convection heat transfer coefficients has been a challenge due to the lack of experimental data in forced convective boiling and condensation of N_2 -hydrocarbon mixtures in liquefaction applications. For instance, Nellis et al. [3] reported experimental data on heat transfer coefficients for mixed refrigerants in a

Joule-Thomson cryocooler. They reported heat transfer coefficients for six boiling mixtures with different molar compositions and operating conditions. Ardhapurkar et al. [4] used their results to test four available boiling heat transfer coefficient correlations. The results show that the correlations proposed by Silver-Bell-Ghaly (S-B-G) and Granryd were suitable to estimate local heat transfer coefficients, although Granryd's correlation was modified to improve accuracy. The same authors [5] also measured single phase, boiling and condensation global heat transfer coefficients for a helically coiled tube-in-tube heat exchanger working with three N₂-Hydrocarbon mixtures, and estimated local heat transfer coefficients with the Dittus-Boelter correlation for single phase, and the modified Granryd correlation for boiling.

Careful review of the literature reveals a lack of experimental and empirical correlations for mixed refrigerant boiling heat transfer, limiting potential for accurate design and sizing of heat exchangers. The difficulty in analyzing boiling of these mixtures has been reported by some authors. For instance, Stephan [6] summarized some physical models available for the estimation of the convective coefficient. Two important features are highlighted after reviewing these models; first, they are based on physical principles, which require great computational effort, and second, they have applicability to phase change of binary, ternary, and multi-component mixtures. However, for practical purposes, researchers mostly use semi-empirical correlations, avoiding the rigorous physical principles involved in heat transfer with phase change. For instance, Celata et al. [7] published a review of empirical and physical methods as a tool to predict the convective coefficient for boiling of binary mixtures. Within the available computational models, empirical models have the advantage of simplicity, contrary to physical models. In addition, some of these empirical models involve physical principles to enable extrapolation.

In recent years, Artificial Neural Networks (ANN) have been used in the field of transport phenomena as a computational tool to develop empirical or semi-empirical models. Particularly in transport phenomena, it is worth mentioning the investigation of Sobowale [8], who simultaneously analyzed heat and mass transfer using an ANN to predict the convective coefficients. Tan et al. [9] developed an ANN for predicting the overall heat transfer rate in compact heat exchangers with water/ethylene glycol anti-freeze mixtures as working fluid and no phase change. Tahavvor and Yaghoubi [10] used ANN techniques to determine natural convection heat transfer and fluid flow around a cooled horizontal circular cylinder with constant wall temperature. Varol et al. [11] developed an ANN model to predict natural convection heat transfer in a triangular enclosure. They did not use experimental information, instead, their study was based on numerical analysis. Tahavvor et al. [12] also modeled natural convection using ANNs. They considered natural convection on a cold horizontal circular cylinder with constant wall temperature. The authors used numerical results for neural network training. Scalabrin and Piazza [13] applied ANNs to forced convection by analyzing carbon dioxide flowing inside a heated tube at supercritical conditions. The model results showed good agreement with experimental information. This model can be considered as semi-empirical because the input variables include the Reynolds, Prandtl, and Eckert numbers. Balcilar et al. [14] used several methods based on artificial intelligence to select the best approach for the prediction of heat transfer coefficient and pressure drop in the condensing flow of R134a. They concluded that the model with the best agreement with experimental data was the multilayer perceptron model with thirteen neurons in the hidden layer. Their model can be classified as empirical because the inputs were directly measured variables such as: mass flux, heat flux, and the difference between the tube wall temperature and the saturation

temperature. Another ANN-based empirical model was proposed by Romero-Mendez [15]. The model predicts the convective heat transfer coefficient associated with the evaporation of a refrigerant inside of mini-tubes. The input variables were: saturation temperature, mass flow rate and heat flux. Thus, it is important to select an appropriate architecture for the model when computational intelligence techniques are used.

This paper proposes three models to estimate the convective heat transfer coefficients during boiling of a multi-component mixture including: nitrogen, methane, ethane, propane and iso-pentane. Since this type of mixture typically boils at cryogenic temperatures, the models have applicability to the sizing of evaporators for natural gas liquefaction plants. The three proposed models are obtained using artificial neural networks, and therefore they are based on computational intelligence. Note that this type of modeling techniques can be extended to the field of two-phase flow, mass and heat transfer, as well as in the field of low temperature technologies such as cryogenics and liquefaction.

The first proposed model is based on directly measured parameters (DMP-ANN) and its inputs are: local quality, local temperature, operating pressure, mass flux and molecular weight. The second model is based on the equivalent Reynolds and Prandtl numbers (eq-ANN) and its inputs are: local quality, equivalent Reynolds number, equivalent Prandtl number and molecular weight. The third model is based on the effective Reynolds and Prandtl numbers (eff-ANN) and its inputs are: local quality, effective Reynolds number, effective Prandtl number and molecular weight. The paper ends with a model validation vs. experimental data not used in the ANN development.

2. Model based on Artificial Neural Networks

Computational models based on artificial intelligence are sophisticated techniques capable of modeling extremely complex processes in diverse areas including pattern recognition, optimization, simulation, and prediction, among others. ANNs are nonlinear systems inspired in biological organisms. Next, a brief review of ANN fundamentals, architecture and operation is presented. For more information, the reader may consult standard references [16,17].

The ANNs used in this paper are feed-forward networks and are organized in clusters of neurons. Each neuron has a weighted connection with all neurons in the neighbor cluster, this connection is represented by a variable called weight (w). Figure 1 shows the structure proposed in this study for the first ANN model. In this case, the model is based on directly measured parameters (DMP-ANN) and the inputs of this model are: local quality, local temperature, operating pressure, mass flux and molecular weight. The output of this model is the convective heat transfer coefficient. The second model (eq-ANN) and the third model (eff-ANN) are very similar to the first model, however, they have four inputs instead of five.

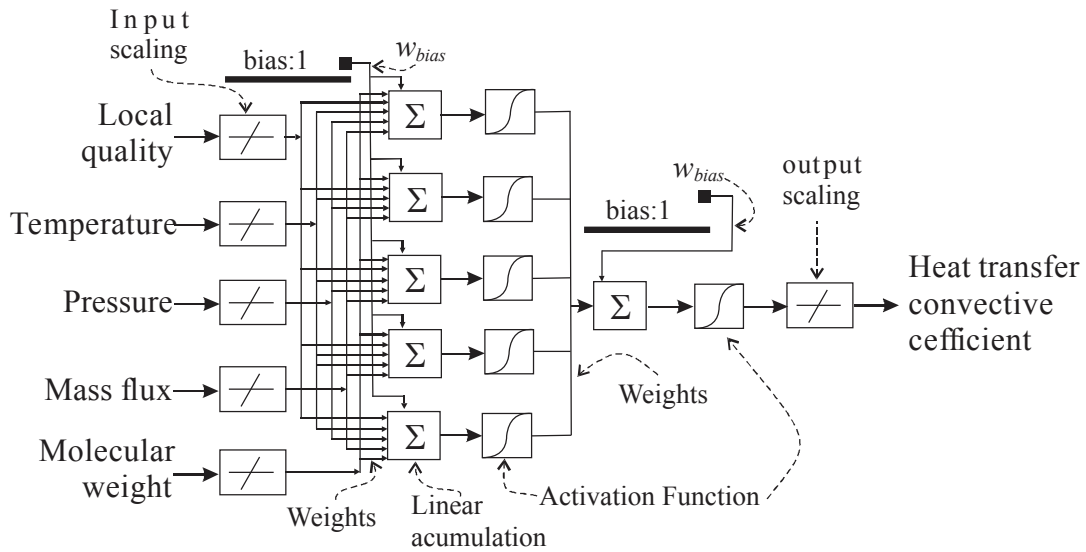


Figure 1. Diagram of the DMP-ANN model.

The network in Figure 1 is considered a black box model because it can be analyzed in terms of its inputs and outputs without any knowledge of its internal workings. However, if all the inputs are directly obtained from measurements, the ANN is deemed purely empirical. Otherwise, if all inputs are associated to physical principles, the ANN is semi-empirical.

Figure 2 shows the k -neuron of an ANN and M represents the number of neurons located in the previous layer. Each neuron combines information by means of a linear accumulation, and then, uses an activation function to produce its output. This function basically executes a nonlinear transformation between the neuron inputs and its output. The activation function used in this paper is defined as: $g(\varepsilon_k) = \tanh(1.5 \varepsilon_k)$. The 1.5 factor in this function has previously been studied, see [18]. The activation function is a very important component of a neuron because it makes the model insensitive to noise.

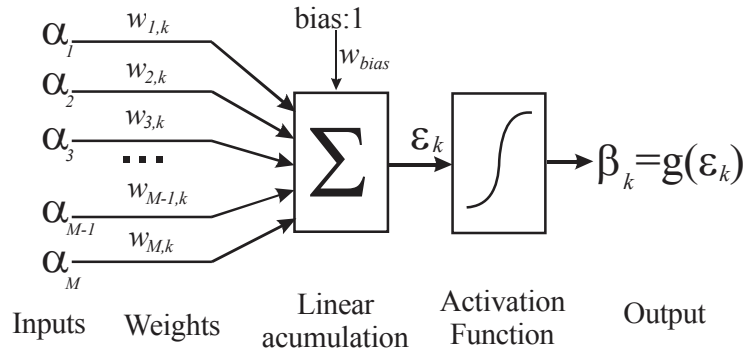


Figure 2. Behavior of an individual artificial neuron.

In biological systems, the learning is stored in neuronal interconnections called synapses. As an analogy, the learning in this computational model is stored in the ANN weights. In Figure 2 each line has an assigned weight (w) which acts as a weighting factor as shown in Eq. 1.

$$\epsilon_k = \sum_{m=1}^M \alpha_m w_{m,k} + w_{bias} \quad (1)$$

In this equation, ϵ is the argument of the activation function. In the proposed model, the training process is responsible for adjusting the weights w , and it requires a data set with input values (α), and a target value (β'). After the training process is completed, an input vector (α) is presented to the network and the ANN produces an output value (β). If β' is close to β for each case, then the learning is considered successful and therefore the performance of the model is acceptable.

An error estimator can be used for determining ANN performance. One typical estimator is the mean relative error, mre , which is computed using the actual network output (β), and the target value (β') as:

$$mre = \frac{1}{N} \sum_{i=1}^N \frac{|\beta_i - \beta'_i|}{\beta'_i} \quad (2)$$

The number of samples used to estimate the *mre* is *N*. Other error estimators can be employed to evaluate the network performance; such as the mean squared error, or the root mean squared error, however, *mre* was chosen because it offers suitable information for this type of application. The next section discusses the experimental details necessary to justify the data set employed for the network development.

3. Experimental information

The experimental information used for development of the ANN models is reported by Nellis et al. [3]. These authors conducted an experimental investigation of forced boiling heat transfer for nitrogen-hydrocarbon mixtures. The publication described a test facility capable of making precise measurements of boiling heat transfer coefficient for a mixed gas working fluid in a microtube at cryogenic temperatures. A vapor mixture with controlled temperature, pressure, mass flux, and composition was introduced into a tube with constant wall temperature and a controlled heating rate. Inlet temperature, outlet temperature and heating power measurements can then be used to calculate the heat transfer coefficient from an energy balance, as indicated by the following equation:

$$\dot{q} = U \cdot LMTD \quad (3)$$

Table 1 shows information from the six experiments performed by Nellis et al. [3]. These experiments include a range of different operating parameters: mixture composition, temperature, mass flux, and pressure. The mixtures for experiments A and B include nitrogen, methane, ethane and propane. Other experiments use: nitrogen, methane, ethane,

propane and iso-butane. The operating pressure for experiments A, B and C was higher than for experiments D, E, and F.

Table 1. Experimental conditions for boiling heat transfer experiments from Nellis et al. [3].

Operating condition	Experiment					
	A	B	C	D	E	F
Molar composition, $N_2/CH_4/C_2H_6/C_3H_8/C_4H_{10}$:	23.3\37\6.8\32.9\0.0	20.4\38.3\5.4\35.8\0.0	7.4\49.4\18.4\17.8\7.0	6.9\50.9\19.1\16.8\6.4	26\38.7\5.4\26.1\3.8	24.1\40.1\5.7\26.3\4.0
Mass flux, $G[kg\ m^{-2}\ s^{-1}]$:	840.5	803.9	767.4	529.9	547.8	255.8
Heat flux, $\dot{q}[kW\ m^{-2}]$:	79.5	79.4	82.7	83.4	82.9	82.9
Pressure, $P[kPa]$:	1365	1439	1424	394	470	434

As our method is based on ANNs, it is necessary to organize the experimental measurements in a data set. Thus, in order to obtain the data sets to train the ANNs of the models proposed in this paper, the plots of Nellis et al. [3] were used. Simple Interactive Object Extraction was used to extract the experimental measurements from the figures, note that this process required little user interaction, see [19]. After applying the extraction algorithm, the data samples from each experiment were merged into a global data set with approximately 1500 samples that includes all information for experiments A-F.

4. Methodology

Once the data set was built, it was split in two: the training set and the validation set. Both sets were stored in digital files for further processing. In this case, it was observed that the percentage rate that provided the best results was 85% of the total data for training, and the remaining 15% for validation. Consequently, each digital file was randomly divided to

create these two files. The computer simulations in this study were performed using the Neural Lab software [20].

It is important in ANN models, whether physical, semi-empirical or empirical, to define the dependent and independent variables. Variables that characterize the fluid and determine the flow can be clearly identified as the independent variables, for instance: quality, temperature, pressure, mass flux and molecular weight. However, the literature shows that the association of these variables produces some dimensionless numbers. For instance, the Nusselt number relates fluid convective and conductive effects, therefore, the convective coefficient appears in Nusselt's mathematical definition, and consequently the Nusselt number is a dependent variable. The independent variables are related to the measurable data, these are: quality (x), Reynolds number (equivalent Re_{eq} and effective Re_{eff}), Prandtl number (the equivalent Pr_{eq} and the effective Pr_{eff}) and molecular weight (MW). Reynolds number relates the flow inertial and viscous effects. Prandtl number relates the thermal diffusivity with the viscous diffusivity. With this in mind, three models are proposed in this investigation: DMP-ANN, eq-ANN and eff-ANN. These models are represented with the following mathematical expressions:

$$h = f(x, T, P, G, MW) \quad (4)$$

$$Nu = f(x, Re_{eq}, Pr_{eq}, MW) \quad (5)$$

$$Nu = f(x, Re_{eff}, Pr_{eff}, MW) \quad (6)$$

where the effective Reynolds, Prandtl and Nusselt numbers are defined as $Re_{eff} = xRe_v + Re_l(1-x)$, $Pr_{eff} = xPr_v + Pr_l(1-x)$, $Nu = hD/k_l$, respectively. These dimensionless numbers are obtained at liquid and vapor phases. On the other hand, the equivalent Reynolds (Re_{eq}), equivalent Prandtl (Pr_{eq}) and Nusselt (Nu) numbers are calculated with

effective properties; $\zeta_{eff} = x\zeta_v + \zeta_l(1-x)$, where ζ represents any transport property that defines the dimensionless numbers as follows: $Re_{eq} = GD / \mu_{eff}$, $Pr_{eq} = (\mu Cp / k)_{eff}$. The Nusselt number for both topologies, Eq. (5) and Eq. (6), is defined as: $Nu = hD/k_l$. Liquid and vapor properties are computed using the REFPROP software [21], and the final black box model is presented in Figure 3. It is important to remark that the three ANN architectures are determined by using all data from experiments A-F. Each of the three models is therefore capable of estimating the convective coefficient (h) or the Nusselt number (Nu) for any of the six experiments.

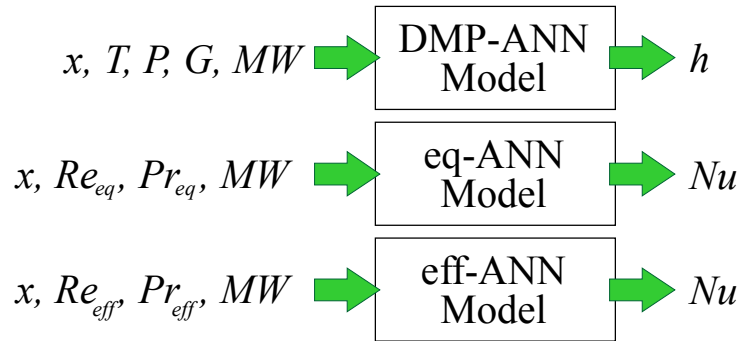


Figure 3. Black box model proposed for the three proposed ANN models.

The internal architecture of the ANN model must be determined using a supervised training method. In this case, two-step training is used. This method consists of a Simulated Annealing step followed by a refining step using the Levenberg Marquardt method. These algorithms and their parameters are presented in Table 2.

Table 2. Algorithm parameters used for the training step.

Simulated annealing	Levenberg Marquardt
Initial temperature=30	Iterations=1000
Final temperature=0.1	<i>mse</i> goal= 10^{-5}
Number of temperatures=100	
Number of iterations per temperature=100	
Cooling schedule=linear	

Simulated Annealing is a technique inspired in the annealing process from metallurgy and it involves controlled heating and cooling of a material [22]. Thus, a substance begins at an initial temperature, and then it is cooled down (linearly or exponentially) until it reaches a final temperature using a specific number of temperatures. The algorithm performs a sequence of iterations at each temperature. In some cases, the algorithm can perform cycles of heating and cooling. These parameters are adjusted to obtain a desired accuracy. This paper, applies a hybrid method using Simulated Annealing and the Levenberg Marquardt method to train the artificial neural network. Simulated Annealing produces an initial solution, and the Levenberg Marquardt method improves the solution found by Simulated Annealing.

The results of this paper are compared with those of Ardhapurkar et al. [4]. These authors verified the applicability of several correlations available in the literature for the prediction of the convective coefficient for flow boiling of N₂-Hydrocarbons mixtures. They recommended the modified Granryd's correlation and the Silver-Bell-Ghaly (S-B-G) method as most suitable to estimate the local heat transfer coefficients. These two models

are analyzed to compare their results with the computed values using the three models proposed in this work. For clarity, the modified Granryd's correlation is included:

$$\frac{h}{h_l} = \frac{Fp}{(1 + A)} \quad (7)$$

where $Fp = 2.37(0.29 + 1/X_{tt})^{0.85}$ and X_{tt} is the Martinelli parameter presented in Eq. 8.

$$X_{tt} = \left(\frac{1-x}{x} \right)^{0.9} \left(\frac{\rho_v}{\rho_l} \right)^{0.5} \left(\frac{\mu_v}{\mu_l} \right)^{0.1} \quad (8)$$

Likewise, h_l is calculated from the correlations of the pure fluids using the properties of the mixture through Eq. 9.

$$h_l = 0.023 \left(\frac{k_l}{D} \right) \left[(1-x) \frac{GD}{\mu_l} \right]^{0.8} \text{Pr}_l^{0.4} \quad (9)$$

And finally, parameter A is obtained with Eq. 10:

$$A = x^2 \left(\frac{Fp}{C} \right) \left[\left(\frac{1-x}{x} \right) \left(\frac{\mu_v}{\mu_l} \right) \right]^{0.8} \left(\frac{\text{Pr}_l}{\text{Pr}_v} \right)^{0.4} \left(\frac{k_l}{k_v} \right) (Cp_v) \left(\frac{\partial h}{\partial T} \right)_p^{-1} \quad (10)$$

In this expression, C is a factor that considers the interface effects between vapor and liquid, and C=2 is recommended for the evaporation of refrigerants. The modified Granryd's correlation suggests C=1.4, if $G > 500 \text{ kg m}^{-2} \text{ s}^{-1}$, and C=2 if $G < 300 \text{ kg m}^{-2} \text{ s}^{-1}$.

For the S-B-G method, the heat transfer coefficient is given by:

$$\frac{1}{h} = \frac{1}{h_l} + \frac{Z}{h_v} \quad (11)$$

where h_l represents the convective coefficient calculated from Eq. 9, h_v is calculated by Dittus-Boelter equation as follows (using the properties of the vapor phase):

$$h_v = 0.023 \left(\frac{k_v}{D} \right) \text{Re}_v^{0.8} \text{Pr}_v^{0.4} \quad (12)$$

Parameter Z is the ratio of the sensible cooling of the vapor to the total cooling rate. It can be obtained by:

$$Z = xC_p \frac{dT_{dew}}{di} \quad (13)$$

where the derivative is the slope of the curve T_{dew} vs. enthalpy of the mixture as it boils.

5. Results and Discussion

Once the model strategy has been presented, it should be developed and discussed. Since there is no specific methodology to choose the number of neurons necessary at hidden layer, a simple program was designed and implemented to compute it. The program starts by creating a neural network with zero neurons in the hidden layer ($\theta=0$), the network is trained with the hybrid scheme previously described, and the mre for validation is computed. The program keeps increasing θ from 0 to 20. Figure 4 shows mre (Eq. 2) as a function of the number of neurons in the hidden layer, for the DMP-ANN model, see Eq. 4. The expression in Eq. 4 suggests that the independent variables are the directly measured parameters.

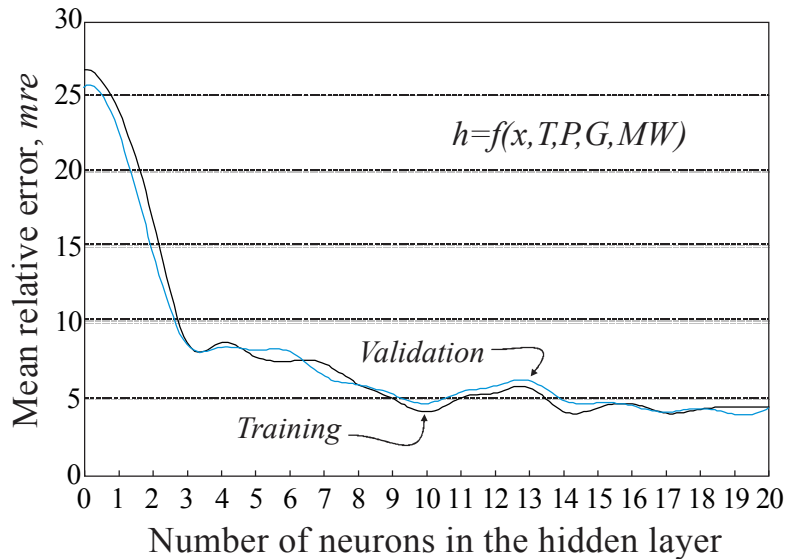


Figure 4. Mean relative error (*mre*) as a function of the number of neurons in the hidden layer, for the DMP-ANN model.

From Figure 4, it can be observed that for zero neurons in the hidden layer, both the training *mre* and the validation *mre* are about 26%. As the number of neurons in the hidden layer θ increases, the *mre* for training and validation decreases. However, little improvement is obtained for $\theta > 10$. Therefore, it is recommended to use 10 neurons in the hidden layer for the DMP-ANN model. Note that this number of neurons provides an accuracy of 4% for training and 4.5% for validation. Note that the error for validation is computed without using the data used for training.

The same procedure is used for the eq-ANN model (Eq. 5). Figure 5 shows the behavior of *mre* when the number of neurons in the hidden layer increases. For $\theta=0$, training and validation *mre* are approximately 27% and 24%. Also, it can be observed that twelve neurons in the hidden layer provides 6.5% *mre* for training and 8% for validation. This number was selected for model evaluation to maintain simplicity and to better reproduce the full weight matrix in Appendix A.

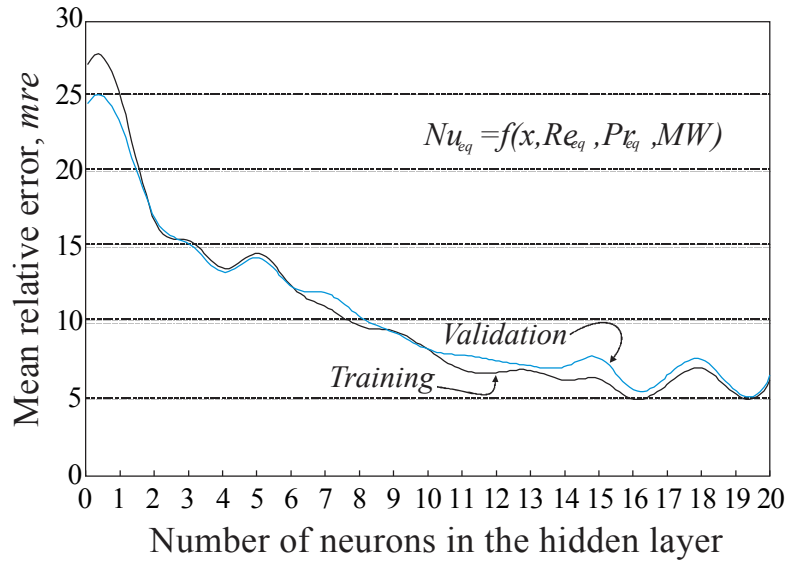


Figure 5. Mean relative error (*mre*) as a function of the number of neurons in the hidden layer, for the eq-ANN model.

Finally, Figure 6 presents the results from eff-ANN (Eq. 6). At the beginning of the simulation, both training and validation *mre* are close to 27%. The optimum number of neurons in the hidden layer (14) can be obtained from inspection of Figure 6. For this number of hidden neurons, the *mre* is 3.5% for training and 4% for validation.

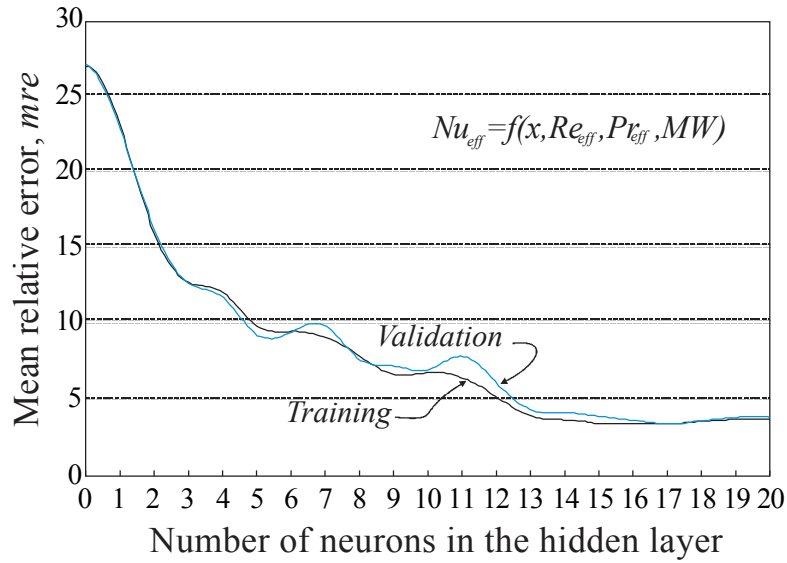


Figure 6. Mean relative error (*mre*) as a function of the number of neurons in the hidden layer, for the eff-ANN model.

Table 3 summarizes the recommended architectures for the estimation of the convective heat transfer coefficient.

Table 3. Recommended architectures for the proposed models.

	Number of neurons			<i>mre</i> [%]	
	Input layer	Hidden layer	Output layer	Training	Validation
DMP-ANN	5	10	1	4	4.5
eq-ANN	4	12	1	6.5	8
eff-ANN	4	14	1	3.5	4

5.1 Comparison of the proposed models with existing models

Once the optimum architecture for each model has been established, the next step is to provide a performance comparison. This comparison includes the three models proposed in this work and two previously demonstrated techniques: the modified Granryd's correlation and the S-B-G method. It is important to mention that the simulations in this work were performed using the recommended architecture of Table 3.

Figure 7 shows a comparison for the convective heat transfer coefficients for experiment A, (Table 1). This figure shows results from the three proposed methods, the modified Granryd’s correlation and the S-B-G method, and experimental data. Observe that the lines in Figure 7 were computed using all experimental data.

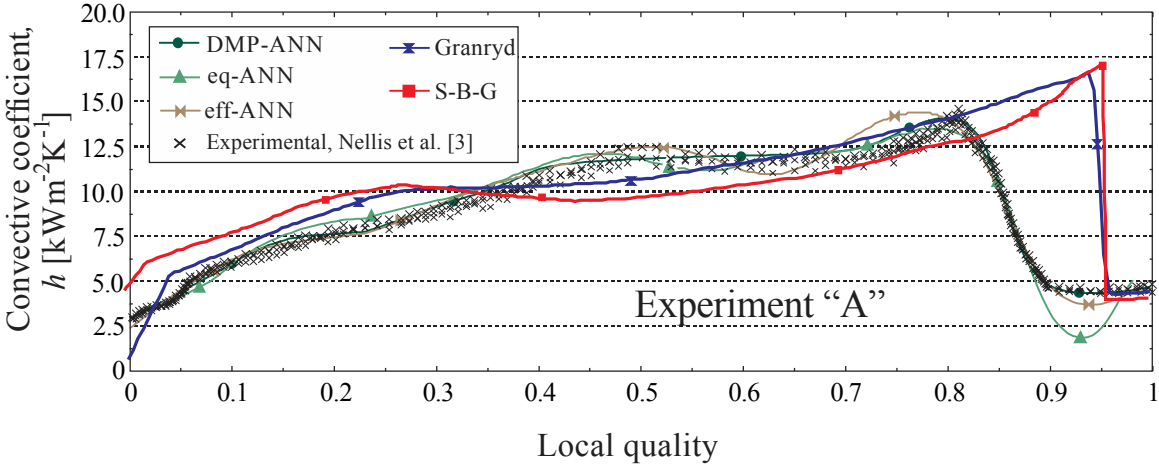


Figure 7. Comparison between experimental and model results for convective heat transfer coefficients for Experiment A.

In Figures 7-12, experimental results are shown in black crosses, DMP-ANN results in dark green line with circles, eq-ANN in light green line with triangles, eff-ANN in olive color line with horizontal arrow heads, Grandryd’s results in dark blue line with vertical arrow heads; and S-B-G results in a red line with squares.

From Figure 7, it can be observed that the Grandryd’s correlation and the S-B-G method predict somewhat similar behavior for the convective heat transfer coefficient when the local quality changes from zero to one. However, these methods exhibit some significant deviations when compared with experimental data, with $mre=66\%$ for Grandryd and $mre=60\%$ for S-B-G. Largest deviations occur for qualities between 0.8 to 0.95, near the end of the boiling process. Figure 7 also reveals that the three proposed models have very

similar behavior to the experimental data. The DMP-ANN model is based on directly measured parameters and shows *mre* of 5.5%. The eq-ANN model resulted in *mre*=6%, note that this model presented a slight discrepancy from the experimental data for local quality in the range from 0.9 to 1. An improvement in the estimations of the heat transfer coefficient is obtained through the eff-ANN model, in this case, the resulting *mre* is only 3.5%. Thus, it can be concluded that the proposed models provide much better accuracy than existing models.

Figure 8 shows a performance comparison for experiment B. The Grandryd correlation and the S-B-G method present considerable deviation from the experimental data, with Grandryd's *mre*=67% and S-B-G's *mre*=87%. The major relative deviation for both models occurs when the local quality is over 0.8. Better estimates are once again obtained from the ANN models. The DMP-ANN model, which is based on directly measured parameters presents *mre*=9.8%. The eq-ANN model, which is based on the equivalent Reynolds and Prandtl numbers produces *mre*=8.9%. The eff-ANN model based on effective Reynolds and Prandtl numbers results in *mre*=5.7%.

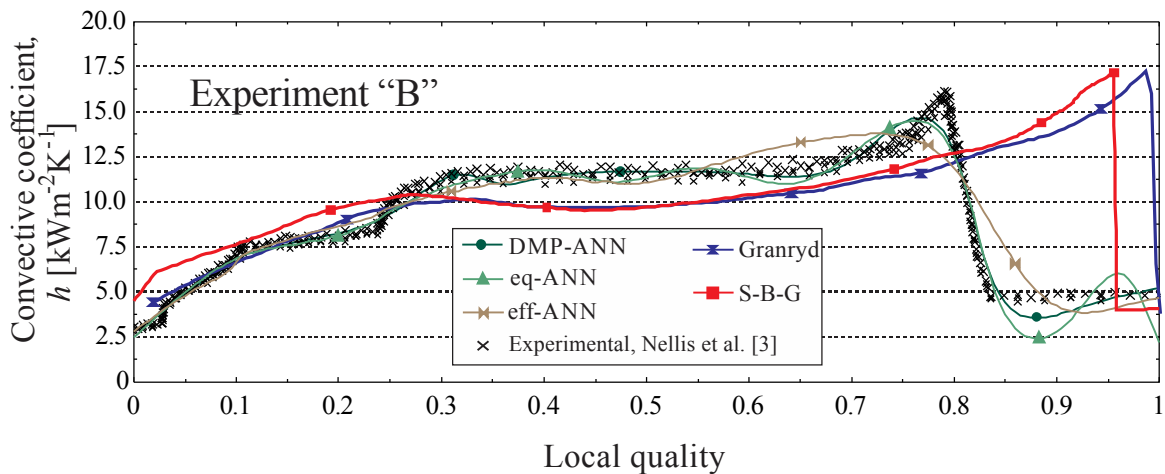


Figure 8. Comparison between experimental and model results for convective heat transfer coefficient for Experiment B.

Figure 9 compares results from experiment C with predictions from the three proposed models, the Grandryd's correlation and the S-B-G method. The figure shows that the three proposed ANN-based models closely predict experimental data, with low $mre=8.7\%$ (DMP-ANN), 3.7% (eq-ANN), and 2.5% (eff-ANN). On the other hand, Grandryd's correlation and the S-B-G method present larger relative deviations of 41.3% and 33.6% . According to Table 1, mass flux, heat flux and pressure did not present significant variations for experiments A, B and C, however, composition is different, since experiment C contains less nitrogen and more propane. It can be concluded that the mre reported by Grandryd's correlation and S-B-G method are highly sensitive to changes in composition; while the proposed ANN models yield similar mre despite the change in composition.

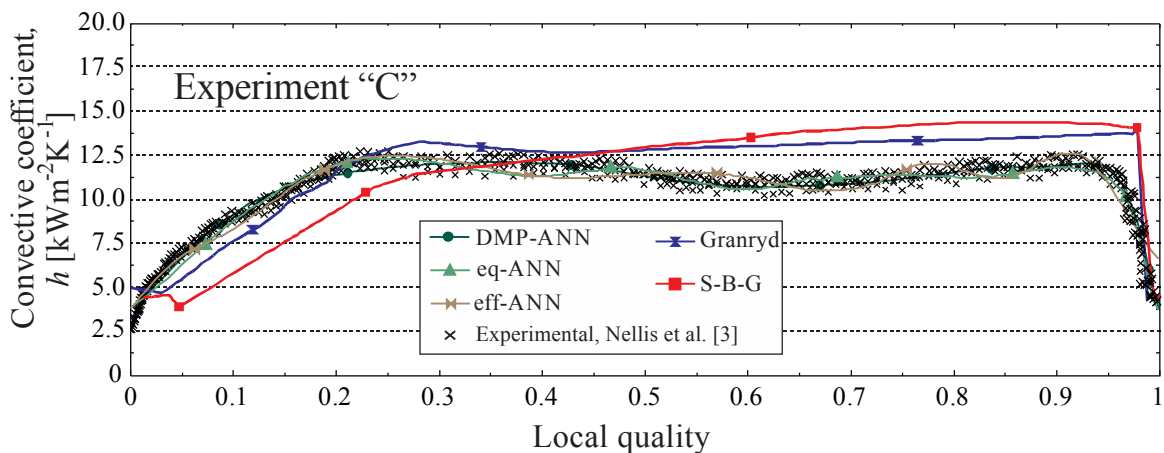


Figure 9. Comparison between experimental and model results for convective heat transfer coefficient for Experiment C.

Table 1 shows that experiments A, B and C were carried out at high pressure, while experiments D, E and F were performed at low pressure. Figure 10 compares results for experiment D. It can be observed that the ANN models show little deviation compared to

Grandryd’s correlation (*mre* 25.8%) and the S-B-G method (*mre* 15.6%). The DMP-ANN model, the eq-ANN model and the eff-ANN model presented *mre*=4.9%, 3.9% and 1.9%. In the five models, the trend of the graphs agrees with experimental data, however, the Grandryd’s correlation and the S-B-G method present large deviations for local quality in the range from 0 to 0.5.

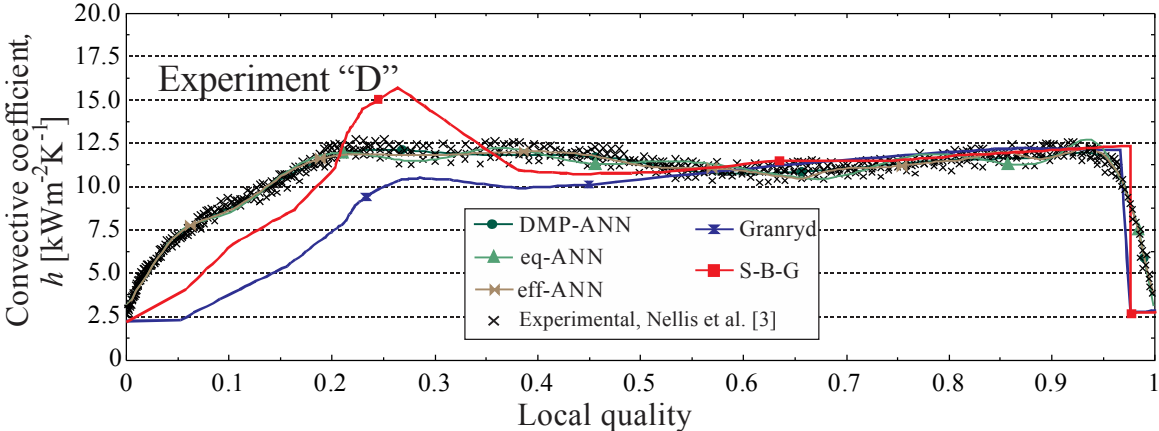


Figure 10. Comparison between experimental and model results for convective heat transfer coefficient for Experiment D.

From the model evaluation for experiment E (Figure 11), it is observed that the Grandryd’s correlation and the S-B-G method present large deviations from experimental data, with relative errors *mre*=42.5% and 30.5%. It is important to note that the S-B-G method presents significant deviation throughout the boiling process, while the Grandryd’s correlation deviates most near the end of the boiling process, for local quality greater than 0.9. As in previous cases, proposed ANN models show better agreement, with DMP-ANN *mre*=5.6%, eff-ANN *mre*=5.9%, and eq-ANN *mre*=8.2%. Some divergence can be seen in Figure 11 between the eq-ANN and the experiment for qualities in the range 0.25 to 0.45, while no major deviations are observed for the DMP-ANN or eff-ANN models.

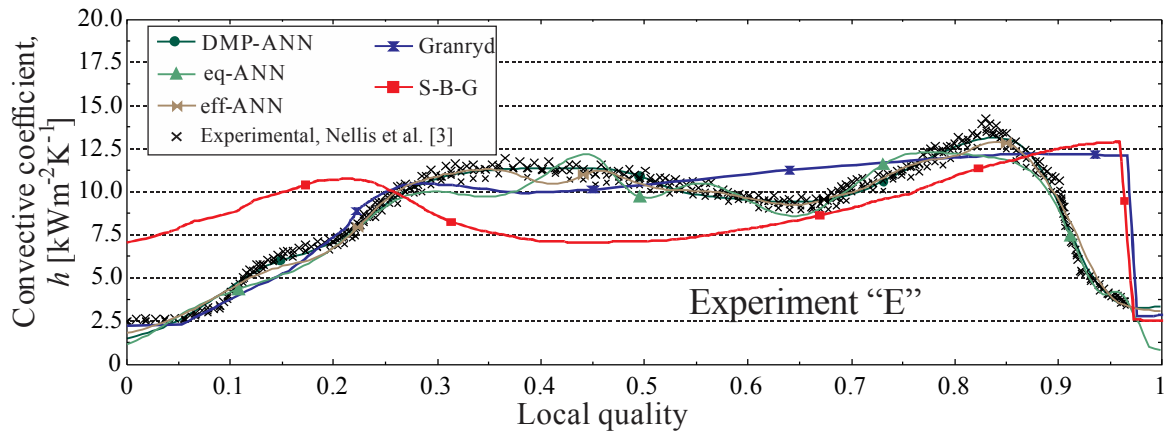


Figure 11. Comparison between experimental and model results for convective heat transfer coefficient for Experiment E.

Finally, the results of experiment F are reported in Figure 12. The models with the largest relative deviations are: the Grandryd’s correlation, the S-B-G method and the eq-ANN model, reporting *mre* values of: 25%, 42.5%, and 14.3%. Similar to Experiment E, the eq-ANN model presents significant deviations for intermediate values of quality, while the DMP-ANN model, with *mre*=11.8%, and the eff-ANN model, with *mre*=8.7%, are most successful at replicating experimental data.

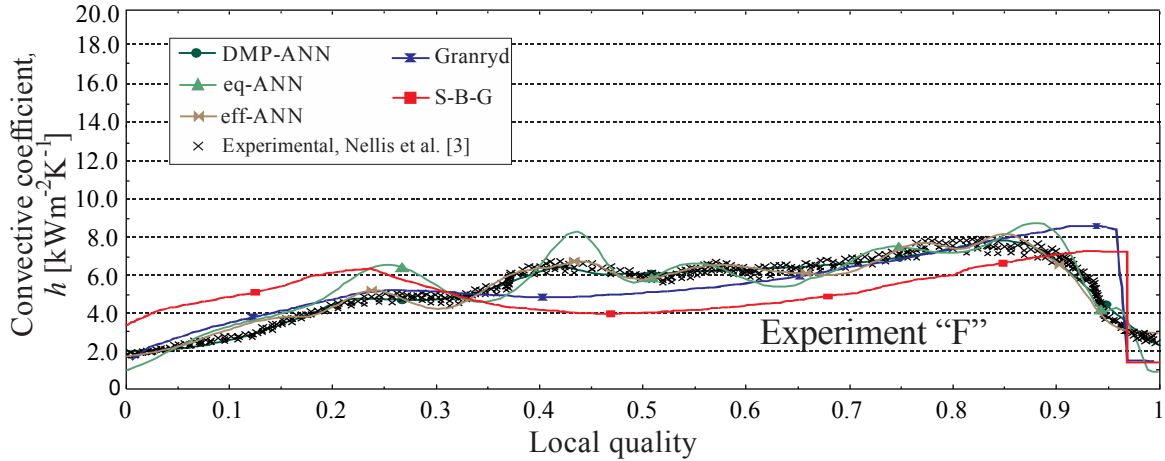


Figure 12. Comparison between experimental and model results for convective heat transfer coefficient for Experiment F.

It can be observed that the proposed models present significant improvements in the prediction of the convective heat transfer coefficient. In particular, eff-ANN produces the best predictions, with the lowest mean relative error $mre=3.9\%$. DMP-ANN is second best with $mre=7.4\%$. From Table 3, it can be seen that these models have very similar number of neurons in the three layers.

The proposed models can be easily implemented within existing programming languages and computing platforms. Appendix A presents the values for the ANN weights (δ) and the algorithm to compute the heat transfer coefficient using the proposed models. It is important to mention that the ranges of the parameters represented by the input layer neurons are: local quality (0-1), operating pressure (394-1439 kPa), local temperature (93.64-276.05 K), mass flux (257-844 $\text{kgm}^{-2}\text{s}^{-1}$), and molecular weight (26.19-29.30 kgkmol^{-1}). It is observed that there is a good distribution of experimental data through the ranges of local quality, temperature, and molecular weight, allowing the DMP-ANN model to learn information corresponding to the behavior in these areas. However, this is not the case for pressure, since of the six experiments, three were done at high pressure and three at

low pressure, and there are no data at intermediate pressures. Caution should therefore be exercised when using the DMP-ANN outside the two pressure ranges: 1365-1439 kPa and 394-470 kPa. In the same way, the DMP-ANN model should be used within the ranges of local quality, temperature and molecular weight that were used for training. On the other hand, the eff-ANN model has fourteen neurons in the hidden layer and extends its range of applicability by having as input the effective Reynolds and Prandtl numbers. For this model, the output neuron corresponds to the Nusselt number for local quality between 0 and 1, effective Reynolds number from 2.22E03 to 7.88E04, effective Prandtl number from 0.79 to 1.82, and molecular weight from 26.19 to 29.30 kgkmol⁻¹.

5.2 Applicability of eff-ANN model to other mixtures

This section compares results from the eff-ANN model vs. experimental data not used in the training step. The eff-ANN model is selected because it is the most accurate (*mre*=3.9% for the six experiments).

Experimental results from Barraza et al. [23] are selected for comparison because they include three experiments that fall within the applicability range shown in Table 3A (Appendix A). Details of the experimental information are shown in Table 4.

Table 4. Experimental conditions for boiling heat transfer experiments from Barraza et al. [23].

Operating condition	Experiment		
	G	H	I
Molar composition, N ₂ \CH ₄ \C ₂ H ₆ \C ₃ H ₈ :	40\27\21\12	20\36\28\16	40\27\21\12
Mass flux, G [kg m ⁻² s ⁻¹]:	144	147	147
Heat flux, \dot{q} [kW m ⁻²]:	57	58	58
Pressure, P [kPa]:	786	791	790

It can be noticed that there are several differences between the experiments in Tables 3 and 4. The main differences between them are the molar composition and the absence or presence of isobutene. Other differences include: lower mass flux, lower heat flux, and intermediate pressure in experiments G-I vs. the pressures used in experiments A-F. However, when calculating the effective-Reynolds, effective-Prandtl and molecular weight, these values are within the eff-ANN applicability range (according to table A3, see appendix A).

Figure 13 shows experimental vs. calculated convective heat transfer coefficient for experiments G (black), H (red) and I (blue). Experimental results are shown with crosses and eff-ANN results with solid lines. The values for *mre* are: 12%, 14% and 7% for experiments G, H and I. Average heat transfer coefficients for experiment G are: 2.69 $\text{kWm}^{-2}\text{K}^{-1}$ measured vs. 2.55 $\text{kWm}^{-2}\text{K}^{-1}$ numerical (*mre* = 5.2%); for experiment H: 3.02 $\text{kWm}^{-2}\text{K}^{-1}$ measured vs. 3.01 $\text{kWm}^{-2}\text{K}^{-1}$ numerical (*mre* = 0.33%), and for experiment I: 2.88 $\text{kWm}^{-2}\text{K}^{-1}$ measured vs. 2.69 $\text{kWm}^{-2}\text{K}^{-1}$ numerical (*mre* = 6.59%), with a global average *mre*=3% for experiments G-I. On the other hand, the average heat transfer coefficients obtained for the eff-ANN model are: 2.55 $\text{kWm}^{-2}\text{K}^{-1}$ (*mre* = 5.2%), 3.01 $\text{kWm}^{-2}\text{K}^{-1}$ (*mre* = 0.33%), and 2.69 $\text{kWm}^{-2}\text{K}^{-1}$ (*mre* = 6.59%), for experiments G, H and I, respectively. Model accuracy is therefore maintained beyond the data set used for ANN development, showing promise toward broad applicability.

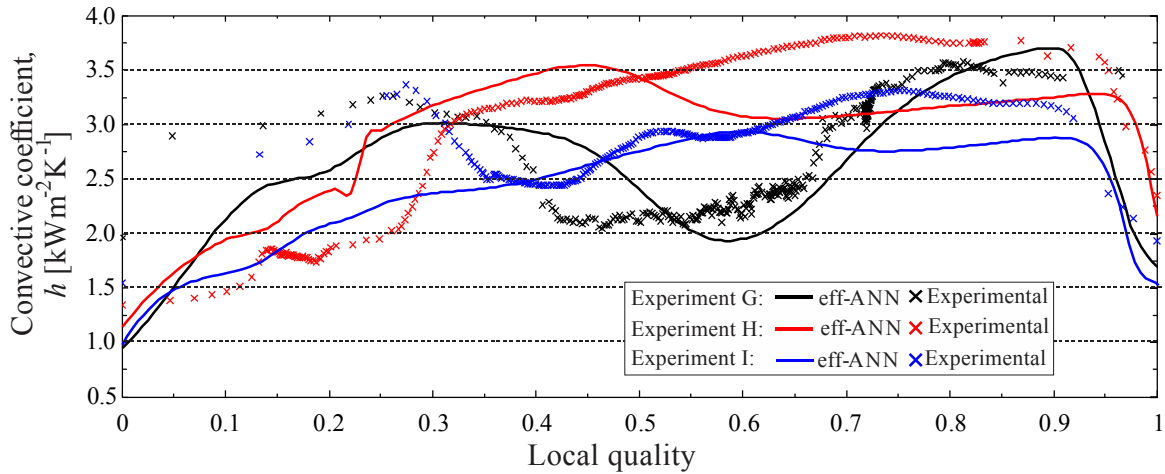


Figure 13. Comparison between experimental and model results for convective heat transfer coefficient for experiments G, H and I.

6. Conclusions

This paper describes the development of three empirical models for predicting boiling heat transfer coefficients for N_2 -hydrocarbon mixtures at cryogenic conditions using computational intelligence techniques. The models are developed with data from six experiments previously published in the literature and tested vs. three additional experiments. The performance of the three proposed models was compared with two existing approaches: Grandry's correlation and the S-B-G method.

The three proposed models are characterized by a set of input variables obtained from experimentation. The DMP-ANN model is based on directly measured parameters and it is the simplest architecture. This model is, however, limited to two relatively narrow pressure ranges: 394-470 kPa and 1365-1439 kPa. The eff-ANN model is based on the effective Reynolds and Prandtl numbers and can be used over broad variable ranges: local quality between 0 and 1, effective Reynolds number between $2.22E03$ and $7.88E04$, effective Prandtl number between 0.79 and 1.82, and molecular weight between 26.19 and 29.30 $kgkmol^{-1}$.

The results demonstrate that the proposed ANN-based approaches greatly outperform available methodologies. While Granryd's correlation predicts experimental data within a mean relative error $mre=44\%$ and the S-B-G method produces $mre=42\%$, DMP-ANN has $mre=7.4\%$ and eff-ANN has $mre=3.9\%$. Considering that eff-ANN has the lowest mean relative error (one tenth of existing models) and the broadest range of applicability, it is recommended for future calculations. The validity of eff-ANN was further tested by comparison with three additional experiments not used in eff-ANN development. Heat transfer coefficients for these experiments were once again well predicted with $mre=11\%$ for local heat transfer and 3% for average heat transfer. Model implementation is straightforward within a variety of platforms and the matrices with the ANN weights are given in the appendix for efficient programming.

Acknowledgements

We thank to Universidad de Guanajuato for the support in the realization of this research. This work performed under the auspices of the U.S. Department of Energy by Lawrence Livermore National Laboratory under Contract DE-AC52-07NA27344.

Declarations of interest

Declarations of interest: none.

References

- [1] W. Lim, K. Choi, Moon, Current Status and Perspectives of Liquefied Natural Gas (LNG) Plant design, Ind. Eng. Chem. Res. 52 (2013) 3065–3088. doi:10.1021/ie302877g.

[2] G.C. Lee, R. Smith, X.X. Zhu, Optimal Synthesis of Mixed-Refrigerant Systems for Low-Temperature Processes, *Ind. Eng. Chem. Res.* 41 (2002) 5016–5028. doi:10.1021/ie020057p.

[3] Nellis G., C. Hughes, J. Pfotenhauer, Heat transfer coefficient measurements for mixed gas working fluids at cryogenic temperatures, *Cryogenics*. 45 (2005) 546–556. doi:10.1016/j.cryogenics.2005.05.002.

[4] P.M. Ardhapurkar, A. Sridharan, M.D. Atrey, Flow boiling heat transfer coefficients at cryogenic temperatures for multi-component refrigerant mixtures of nitrogen–hydrocarbons, *Cryogenics*. 59 (2014) 84–92. doi:10.1016/j.cryogenics.2013.11.006.

[5] P.M. Ardhapurkar, A. Sridharan, M.D. Atrey. Performance evaluation of heat exchanger for mixed refrigerant J–T cryocooler. *Cryogenics*. 2014; 63:49–56. doi:10.1016/j.cryogenics.2014.06.012.

[6] K. Stephan, *Heat transfer in condensation and boiling*, Springer-Verlag, Berlin Heidelberg, 1992. doi:10.1007/978-3-642-52457-8.

[7] G.P. Celata, M. Cumo, T. Setaro, A review of pool and forced convective boiling of binary mixtures, *Exp. Therm. Fluid Sci.* 9 (1994) 367–381. doi:10.1016/0894-1777(94)90015-9.

[8] S.S. Sobowale, S.O. Awonorin, T.A. Shittu, E.S.A. Ajisegiri, Artificial Neural Network (ANN) of Simultaneous Heat and Mass Transfer Model during Reconstitution of Gari Granules into Thick Paste, *Int. J. Chem. Eng. Appl.* 5 (2014) 452–457. doi:10.18178/IJCEA.

- [9] C.K. Tan, J. Ward, S.J. Wilcox, R. Payne, Artificial neural network modelling of the thermal performance of a compact heat exchanger, *Applied Thermal Engineering* 29 (2009) 3609–3617. doi:10.1016/j.applthermaleng.2009.06.017.
- [10] A.R. Tahavvor, M. Yaghoubi, Analysis of natural convection from a column of cold horizontal cylinders using Artificial Neural Network, *Appl. Math. Model.* 36 (2012) 3176–3188. doi:10.1016/j.apm.2011.10.003.
- [11] Y. Varol, E. Avci, A. Koca, H. Oztop, Prediction of flow fields and temperature distributions due to natural convection in a triangular enclosure using Adaptive-Network-Based Fuzzy Inference System (ANFIS) and Artificial Neural Network (ANN), *Int. Commun. Heat Mass Transf.* 34 (2007) 887–896. doi:10.1016/j.icheatmasstransfer.2007.03.004.
- [12] A.R. Tahavvor, M. Yaghoubi, Natural cooling of horizontal cylinder using Artificial Neural Network (ANN), *Int. Commun. Heat Mass Transf.* 35 (2008) 1196–1203. doi:10.1016/j.apm.2011.10.003.
- [13] G. Scalabrin, L. Piazza, Analysis of forced convection heat transfer to supercritical carbon dioxide inside tubes using neural networks, *Int. J. Heat Mass Transf.* 46 (2003) 1139–1154. doi:10.1016/S0017-9310(02)00382-4.
- [14] M. Balcilar, A.S. Dalkilic, S. Wongwises, Artificial neural network techniques for the determination of condensation heat transfer characteristics during downward annular flow of R134a inside a vertical smooth tube, *Int. Commun. Heat Mass Transf.* 38 (2011) 75–84. doi:10.1016/j.icheatmasstransfer.2010.10.009.

- [15] R. Romero-Méndez, P. Lara-Vázquez, F. Oviedo-Tolentino, H.M. Durán-García, F.G. Pérez-Gutiérrez, A. Pacheco-Vega, Use of Artificial Neural Networks for Prediction of the Convective Heat Transfer Coefficient in Evaporative Mini-Tubes, *Ing. Investig. Y Tecnol.* 17 (2016) 23–34. doi:10.1016/j.riit.2016.01.003.
- [16] S.J. Russel, P. Norvig, *Artificial Intelligence: A Modern Approach*, in: Prentice Hall, Upper Saddle River, NJ, USA, 2009.
- [17] M.T. Jones, *Artificial Intelligence: A Systems Approach*, in: Infinity Science Press LLC, Massachusetts, 2008.
- [18] T. Masters, *Practical Neural Network Recipes in C++*, Academic Press, Inc, San Diego, CA., 1993.
- [19] G. Friedland, K. Jantz, R. Rojas, SIOX: Simple Interactive Object Extraction in Still Images, in: *Seventh IEEE Int. Symp. Multimed.*, IEEE, 2005: pp. 253–260. doi:10.1109/ISM.2005.106.
- [20] S. Ledesma, D.L. Ibarra-Manzano, M.A., Garcia-Hernandez, M.G., Almanza-Ojeda, Neural Lab a Simulator for Artificial Neural Networks, in: *IEEE Comput. Conf.*, 2017: pp. 716–721.
- [21] E. W. Lemmon, M. L. Huber, M. O. McLinden, NIST's Standard Reference Database 23: Reference Fluid Thermodynamic and Transport Properties-REFPROP, National Institute of Standards and Technology, Standard Reference Data Program, Gaithersburg, 2007.

[22] W.H. Press, S. Teukolsky, W.T. Vetterling, F. B.P., Numerical Recipes: The Art of Scientific Computing, Cambridge University Press, 2007.

[23] Barraza R, Nellis G, Klein S, Reindl D. Measured and predicted heat transfer coefficients for boiling zeotropic mixed refrigerants in horizontal tubes. Int. J Heat Mass Transf 2016;97:683–95. doi:10.1016/j.ijheatmasstransfer.2016.02.030.

Appendix A

This appendix presents the basis methodology to implement the proposed algorithm in any programming language. This methodology is independent of the architecture of the neural network. The first step is selecting one of the three developed architectures. The second step is creating a vector associated with the chosen architecture and the physical conditions necessary for estimating the convective heat transfer coefficient. For the DMP-ANN model, the vector is composed of the following information: quality, temperature, pressure, mass flux and molecular weight. For the eq-ANN model, the vector is composed of: quality, equivalent Reynolds (Re_{eq}), equivalent Prandtl (Pr_{eq}), and molecular weight. These numbers are calculated with effective properties; $\zeta_{eff} = x\zeta_v + \zeta_l(1-x)$, where ζ represents any transport property that defines the dimensionless numbers as follows: $Re_{eq} = GD / \mu_{eff}$, $Pr_{eq} = (\mu Cp / k)_{eff}$. For the eff-ANN model, the vector is composed of: quality, effective Reynolds (Re_{eff}), effective Prandtl (Pr_{eff}), and molecular weight. These numbers are defined as $Re_{eff} = xRe_v + Re_l(1-x)$, $Pr_{eff} = xPr_v + Pr_l(1-x)$. The subscripts v and l are obtained at liquid and vapor phases.

Once the architecture is selected and its corresponding vector input is created, the third step is identifying the maximum and minimum values of the inputs and outputs for the chosen configuration. Table 1A, 2A and 3A present these values for the DMP-ANN, eq-ANN and eff-ANN models. The main purpose of this step is normalizing the all input values to the range -1 to 1, i.e., the minimum input value must be mapped to -1 and the maximum to 1. Similarly, the output values, commonly known as target values, must be scaled to the range from -0.9 to 0.9 [16].

Table 1A. Limiting values of the input variables and output parameters for the DPM-ANN model.

	Quality [-]	Pressure [kPa]	Local temperature [K]	Mass flux [kgm ⁻² s ⁻¹]	Molecular weight [kgkmol ⁻¹]	Heat transfer coefficient [kWm ⁻² K ⁻¹]
Minimum limit	0	394	93.64	2.57E02	26.19	1.776
Maximum limit	1	1439	276.06	8.44E02	29.30	15.730

Table 2A. Limiting values of the input variables and output parameters for the eq-ANN model.

	Quality [-]	Equivalent Reynolds number [-]	Equivalent Prandtl number [-]	Molecular weight [kgkmol ⁻¹]	Nusselt number [-]
Minimum limit	0	2.22E03	0.79	26.19	7.48
Maximum limit	1	7.46E04	2.90	29.30	77.24

Table 3A. Limiting values of the input variables and output parameters for the eff-ANN model.

	Quality [-]	Effective Reynolds	Effective Prandtl	Molecular weight	Nusselt number [-]
--	----------------	-----------------------	----------------------	---------------------	-----------------------

		number [-]	number [-]	[kgkmol ⁻¹]	
Minimum limit	0	2.22E03	0.79	26.19	7.48
Maximum limit	1	7.88E04	1.82	29.30	77.24

The fourth step consists of executing the following matrix operation:

$$\sigma = \tanh\left(1.5 \left[\delta_2 \cdot \left[\tanh\left(1.5 \left[\delta_1 \cdot [\Phi; 1] \right] \right); 1 \right] \right] \right) \quad (1A)$$

Where δ is the weight matrix defined at the end of this appendix for the three models, these matrices represent the weights of the hidden and output layers. Thus, these matrices were computed during the training step of the ANN. Likewise, Φ is a column vector that represents the normalized scaled inputs obtained in step three. In Eq. 1A, the semicolon represents the addition of a row, whose element is a vector with ones (this vector represents the input typically known as BIAS). The output of this equation is represented by σ and has a value between -0.9 to 0.9; therefore, the third step is to scale this value back to the domain of the corresponding output, in this case, the minimum and maximum values of the Nusselt number or the convective coefficient (depending on the network chosen in the first step). The evaluation of Eq. 1A can be performed using any software that supports vector operations, such as: Matlab, Neural Lab, Software-R, Microsoft Excel, etc.

For the DMP-ANN model, the matrices δ_1 and δ_2 are defined as:

$$\delta_1 = \begin{bmatrix} -0.59140 & -0.07399 & -0.06893 & 0.12848 & 0.03115 & -1.37423 \\ -1.29867 & -0.88545 & -1.85121 & 2.70831 & -5.03427 & 1.21363 \\ 9.41699 & -0.04050 & -5.19773 & 1.44787 & 1.72570 & -4.74123 \\ 4.02992 & 3.87909 & 0.27248 & 2.82836 & 2.08628 & -0.70505 \\ -2.04763 & -2.54915 & 2.90319 & 1.01828 & -1.41025 & -2.4751 \\ 9.20554 & 3.01382 & 1.93570 & -0.6932 & -4.94957 & -11.2157 \\ -10.5255 & 4.91713 & -0.84483 & 6.83200 & 2.33582 & -2.9644 \\ -1.59610 & -3.38629 & 1.04636 & 1.61590 & -3.71274 & -3.6505 \\ 2.10514 & -4.26096 & -5.63363 & 3.95239 & -4.68736 & -5.2999 \\ -1.23133 & -1.33686 & 0.54627 & -3.76812 & 0.99325 & -3.2288 \end{bmatrix}$$

$$\delta_2 = [-4.46799 \quad -0.044580 \quad -0.90162 \quad 0.43075 \quad -1.68845 \quad -0.91160 \quad \dots \\ \dots \quad -0.45977 \quad -1.68747 \quad 3.33005 \quad -0.32149 \quad -6.16379]$$

For the eq-ANN model, the matrices δ_1 and δ_2 are defined as:

$$\delta_1 = \begin{bmatrix} 0.65026 & 1.16076 & -1.09086 & -3.31321 & -0.69582 \\ 1.93904 & 1.66230 & 0.51696 & -1.40964 & 1.44250 \\ -1.05303 & -2.11040 & -0.52918 & 1.22859 & -1.41290 \\ 1.11207 & 1.07960 & -2.94240 & 1.25355 & -0.77444 \\ -2.77537 & -1.77970 & 1.72808 & -1.36384 & -2.26014 \\ -1.44317 & -0.10365 & 0.56507 & 0.57131 & 0.42936 \\ 2.06820 & 1.82863 & -0.45875 & 2.53341 & -0.74027 \\ -0.99859 & -3.89480 & 0.63245 & 1.18776 & 0.98039 \\ 6.78296 & 6.21511 & 1.61528 & 2.34200 & -2.12333 \\ 0.31902 & -5.90821 & -0.71421 & 2.28270 & -7.02692 \\ 2.11925 & 0.10528 & -3.26467 & 0.25063 & 2.59801 \\ 6.28485 & 5.42689 & 1.53305 & 1.91737 & -2.17017 \end{bmatrix}$$

$$\delta_2 = [0.11987 \quad -0.51788 \quad -1.00603 \quad 0.08614 \quad -0.37208 \quad 0.85843 \quad 0.15079 \quad \dots \\ \dots \quad -0.10561 \quad 2.37471 \quad -1.85821 \quad 2.01667 \quad -2.88516 \quad -4.13985]$$

For the eff-ANN scheme, the matrices δ_1 and δ_2 are defined as:

$$\delta_1 = \begin{bmatrix} -3.44995 & -1.59721 & 3.26466 & -4.10155 & 6.05694 \\ -1.64313 & -1.08043 & -1.30051 & 2.74094 & 0.25049 \\ -1.29137 & 1.40011 & 1.28959 & -0.90959 & -2.38171 \\ 3.27904 & -1.75167 & 0.83503 & 0.57314 & -0.65348 \\ 0.27894 & -1.15111 & 0.51991 & 2.52208 & 1.96872 \\ 0.43887 & 2.64878 & 0.43180 & -0.08493 & -0.60518 \\ -1.92862 & -0.46487 & -0.21424 & 1.49685 & -0.01645 \\ 0.03832 & -2.14198 & 0.45289 & 0.04922 & -2.06448 \\ -0.38745 & 2.61082 & -2.31006 & -1.21979 & 1.12817 \\ 0.26273 & 2.84053 & -0.37332 & 0.63547 & 2.61472 \\ -0.48691 & 0.64478 & 0.36396 & -1.01985 & 0.07839 \\ 0.66957 & -0.95126 & 2.45821 & -1.40772 & 0.86900 \\ 0.67090 & -1.21825 & 3.13382 & -2.19225 & 1.73345 \\ -1.06291 & -0.34953 & 1.21712 & 0.96194 & 1.43636 \end{bmatrix}$$

$$\delta_2 = [1.36257 \quad -0.52023 \quad -1.34565 \quad -0.38097 \quad -0.23220 \quad 0.056380 \quad 0.29958 \quad -1.80051 \quad \dots \\ \dots \quad 0.25445 \quad -0.944894 \quad -0.896735 \quad 1.35839 \quad -2.26857 \quad 0.143925 \quad -2.13834]$$